



Title	Tough Hydrogels with Fast, Strong, and Reversible Underwater Adhesion Based on a Multiscale Design
Author(s)	Rao, Ping; Sun, Tao Lin; Chen, Liang; Takahashi, Riku; Shinohara, Gento; Guo, Hui; King, Daniel R.; Kurokawa, Takayuki; Gong, Jian Ping
Citation	Advanced Materials, 30(32), 1801884 https://doi.org/10.1002/adma.201801884
Issue Date	2018-08-09
Doc URL	http://hdl.handle.net/2115/75191
Rights	This is the peer reviewed version of the following article: Ping Rao Tao Lin Sun Liang Chen Riku Takahashi Gento Shinohara Hui Guo Daniel R. King Takayuki Kurokawa Jian Ping Gong, Tough Hydrogels with Fast, Strong, and Reversible Underwater Adhesion Based on a Multiscale Design, Advanced materials, 2018, 30, 1801884. which has been published in final form at https://doi.org/10.1002/adma.201801884 . This article may be used for non-commercial purposes in accordance with Wiley Terms and Conditions for Use of Self-Archived Versions.
Type	article (author version)
Additional Information	There are other files related to this item in HUSCAP. Check the above URL.
File Information	Supplementary Information-adma.201801884.pdf (Supplementary Information)



[Instructions for use](#)

Supplementary Information

Tough hydrogels with fast, strong, and reversible underwater adhesion based on a multi-scale design

Ping Rao¹, Tao Lin Sun^{2,3,4}, Liang Chen¹, Riku Takahashi¹, Gento Shinohara⁵, Hui Guo², Daniel R. King^{2,3}, Takayuki Kurokawa^{2,3}, and Jian Ping Gong^{2,3}*

P. Rao, L. Chen, R. Takahashi,

¹Graduate School of Life Science, Hokkaido University, Sapporo 001-0021, Japan.

Dr. T. L. Sun, Dr. H. Guo, Dr. D. R. King, Prof. T. Kurokawa, Prof. J. P. Gong,

²Faculty of Advanced Life Science, Hokkaido University, Sapporo 001-0021, Japan.

Dr. T. L. Sun, Dr. D. R. King, Prof. T. Kurokawa, Prof. J. P. Gong,

³Global Institution for Collaborative Research and Education (GI-CoRE), Hokkaido University, Sapporo 001-0021, Japan.

Dr. T. L. Sun,

⁴South China Advanced Institute for Soft Matter Science and Technology, South China University of Technology, Guangzhou 510640, China.

G. Shinohara,

⁵Department of Zoology, National Museum of Nature and Science, Tsukuba 305-0005, Japan.

Prof. J. P. Gong

* Corresponding Author, Email: gong@sci.hokudai.ac.jp

1. Methods

1) Synthesis of PA patterned hydrogels. The tough polyampholyte (PA) hydrogels were prepared by the random copolymerization of NaSS and DMAEA-Q at a NaSS : DMAEA-Q monomer ratio of 0.52 : 0.48, as described in previous studies.^[1] An aqueous solution containing 2.5 M total monomer concentration, 2.5 mM, 2-oxoglutaric acid as UV initiator, and 2.5 mM *N,N*-methylenebisacrylamide crosslinker was poured into a reaction cell consisting of a piece of fresh glass plate and a piece of silicone mold separated by a silicone spacer of prescribed thickness. Then the reaction cell was irradiated with 365 nm UV light for 10 h. To remove the oxygen, the silicone mold and spacer were placed in an Ar atmosphere before use for more than 36 h. After polymerization, the gel was immersed in excess amount of water for 1 week to dialyze the mobile counter-ions, and allow the oppositely charged polyions on the copolymers to form stable ionic complexes through intra- or inter-chain interactions. The PA gel deswelled to 87.5% of its as-prepared size in each direction after dialysis, and became very tough.

To induce surface groove features, the gelation of the PA gels was performed in a rectangular reaction cell with a $t'=2.0$ mm thick spacer where one cell wall was made from a silicone mold with honeycomb-like grid structure (Figure S5). The width (w') and height (h') of the grid molds were kept constant at 0.75, and 0.5 mm, respectively, while the hexagon side length (a') of the ridge varied from 1 to 2 mm. By using this method, we obtained PA gels with flat hexagonal facets separated by interconnecting grooves. The size of the grooves on the PA gel surface was tailored using the grid of the mold and the total thickness of the gel using the silicone spacer, but all these sizes were reduced to 87.5% due to the deswelling of the gel by dialysis.

2) Synthesizing hydrogels with hydrogen bonds. The tough P((PEG)₂₀₀OMe-co-AAc) hydrogels (denoted as POA gels) with hydrogen bonds were prepared using the random copolymerization of the poly(ethylene glycol)₂₀₀ monomethyl ether monomethacrylate ((PEG)₂₀₀OMe) macromer, and acrylic acid (AAc) monomer with a 1.5 molar ratio of PEG segments in (PEG)₂₀₀OMe to pendant carboxylic acids in AAc. The POA hydrogels were prepared using the same procedure as the polyampholyte (PA) hydrogels from a dimethyl sulfoxide (DMSO) solution containing 2 M in total macromer and monomer, and 2 mM 2-oxoglutaric acid as UV initiator. After the gelation, the POA hydrogels were immersed in water to remove the DMSO and allow the forming of hydrogen bonds. The POA hydrogels deswelled to 81% of their as-prepared size in each direction in water.

3) *In situ* observation of the underwater contact formation evolution. Underwater contact formation evolution was observed using a homemade system as shown in Figure 2b. The observation was based on the critical refraction principle.^[2-4] Since the hydrogel has a smaller refractive index than glass, but a slightly larger one than water, the light from the gel side reflects at angles between the critical angles of glass and water. A light image is observed when the gel is in contact with the substrate, and a black image when water drops exist at the interface. A 35 mm diameter disc shaped gel (flat or patterned) was placed on a plastic substrate in the stage box filled with water. An isosceles trapezoidal prism (angle 70°, length 66 mm, height 22.08 mm, and width 50 mm), attached to the load cell using a rigid holder, approached the gel from the top at a steady 10 μm/s rate until the force reached the designed 15 N value. At the same time, the contact image of the gel on the prism surface was observed from an angle between the critical angles of water and gel using a zoom camera. The evolution of the contact image in time was subsequently recorded at the fixed displacement for different samples (see Movie S1, Supplementary Information). The contact areas for these

snapshots at different times were calculated using the Image-J software, and the contact area ratios were calculated respective to the nominal area of the flat sample or the hexagonal pads area of the patterned gels.

4) Underwater probe tack test. The probe tack tests, for measuring the adhesion strength and energy dissipation of the hydrogels, were performed on a Shimadzu Autograph AG-X 20KN tensile machine in water at 25 °C. The set-up consisted of mainly two parts (Figure 6, Supplementary Information): the bottom part, a cell with a rigid stage providing the deionized water environment for the tack test, and the upper one, a copper shaft connected with the load cell. The gel was cut into disc shapes of prescribed diameter, and bonded to the copper shaft using a very thin super glue (Konishi Co., Ltd.). We used copper plate, glass plate, polystyrene, flat gel, and pork heart tissue glued to the glass plate as counter substrates. The copper and glass plate we used were first washed by acetone and then washed by deionized water. The glass used was micro slide glass made by the MATSUNAMI Company of Japan (product number S2112). The glass carried negative surface charges, and the Zeta potential measured in 10 mM sodium chloride (NaCl) aqueous solution was -32.44 mV, measured by the Zeta potential and Particle size analyzer (ELSZ-2000, Otsuka Electronics Co., Ltd (Osaka, Japan)). The contact angle to water was $19.6 \pm 2.2^\circ$ at 25 °C. Polystyrene used for Petri dish is made by the IWAKI Company of Japan. Fresh pork heart, beef heart were purchased from Nippon Food Packer Inc. (Japan) and used as received without any surface pretreatment. Then the substrate was directly secured to the stage using a hard cover with screws. Before starting to measure, both parts were immersed in water and we waited for 30 min for the equilibrium state to be reached.

For the test, the upper gel was first compressed to the lower substrate at a constant compressing rate until it reached the set force (F). Afterward, the sample was held in this

position for the described contact time (t). Subsequently, the probe was retracted at a constant rate until the debonding finished. The force, displacement, and time were recorded during the process.

5) Rheological test. The rheological test was performed using an advanced rheometric expansion system (ARES) (Rheometric Science Inc.). A disc sample with a 15 mm diameter and a 2.5×0.875 mm thickness, was glued between the metal plates and surrounded by water. A rheological frequency sweep from 0.01 to 100 rad/s was performed at a constant strain of 0.1% and at temperature of 25 °C.

6) Underwater tensile test. The tensile test was performed using a tensile-compressive tester (TENSILON ORIENTEC RTC-1150A) underwater at 25 °C. The sample was cut into a Dumbbell-shape with the JIS-K6251-7 standard size: $6 \times 2 \times 2$ mm³. The tensile velocity was 100 mm/min, corresponding to a 0.28 s^{-1} strain rate. The nominal stress was obtained by dividing the tensile force by the initial cross-sectional area of the sample.

7) Underwater hysteresis test. The hysteresis test was performed using the same set-up and sample size as the underwater tensile test. The sample was first stretched to the designed critical strains $\varepsilon = 3, 6, \text{ and } 8$, respectively with a 0.28 s^{-1} strain rate, followed by immediately unloading the sample to the original clamp position at the same loading-unloading velocity without waiting at the prescribed stretch peak. After the sample was held in this position for a waiting period, t , it was stretched to the same extension ratio, λ , and returned to the original position again, completing the second cycle. Subsequent tensile cycles were performed for various waiting times between two adjacent cycles. Hysteresis or energy dissipation was calculated from the area enclosed by the loading-unloading curve. The hysteresis ratio is calculated by hysteresis after the first loop divided by the hysteresis of the virgin samples.

8) Preparation of the silicone mold. A plastic mold (10×10 cm) with a concave honeycomb pattern was prepared using a 3D Keyence printer. The hexagonal honeycomb concave areas with a side length of 1 or 2 mm were separated by 0.5 mm high and 0.75 mm wide grooves. The mixed two-part polymers with 0.5 wt.% silicone solution curing agent for silicone rubbers was cased into the plastic mold, and the sample was placed in a vacuum chamber for 30 min to remove the bubbles. Subsequently, the sample was exposed to the moisture in the air at 25 °C for 24 h for curing the silicone rubber. After removing the plastic mold, we obtained a 5 mm thick silicone mold with honeycomb-like surface ridges, and the dimension of the ridge are 0.5 mm height (h'), 0.75 mm width (w') and 1 or 2 mm hexagonal side length (a').

2. Legends for Supplementary Movies

Movie S1

Underwater contact evolution of PA hydrogels on glass.

We recorded the contact area evolution of the flat P0, patterned P1, and P2 hydrogels on a glass prism surface in time. The display speed is 8 times faster than real time at the beginning and 128 times faster for the long drainage time for each sample.

Movie S2

Underwater adhesion of patterned PA hydrogels on hard glass.

A strip of patterned PA hydrogel was immersed in Milli-Q water. Subsequently we pressed a piece of slide glass on one end of the patterned gel strip with one finger, and another piece of

glass plate on the other end of patterned gel. The two pieces of slide glass plate adhered to the patterned gel very well. We finally stretched the adhesion joints, and observed that the tough hydrogel was significantly stretched and presented considerable deformation. However, for the flat PA hydrogel, while the glass plate can adhere underwater, the adhered joint was very weak and failed quickly.

Movie S3

Underwater self-adhesion of patterned PA hydrogels.

A strip of P1 patterned PA hydrogel was cut into two pieces in Milli-Q water. Furthermore, we placed the flat surface ends of the two strips in contact underwater, and stretched the joint. While the flat surfaces could adhere to each other, they showed weak adhesion. Subsequently, we placed the patterned surface ends of the two strips in contact underwater, and stretched the joint. The gels could adhere to each other, but also showed weak adhesion. Lastly, when the end of a patterned surface strip was attached to the end of a flat surface strip we noticed that the joint could be substantially stretched and bear large deformation.

Movie S4

Underwater adhesion of patterned PA hydrogels to bio-tissue.

A piece of beef heart was placed underwater and a strip of P1 patterned PA hydrogel was pressed to the tissue using tweezers and very little pressure. While we immediately dragged the tissue underwater and even flipped it upside down, the patterned hydrogel still strongly adhered to the tissue. Afterward, we took the tissue out of the water holding the corner of the

patterned hydrogels with the tweezers. This movie clearly showed the fast and strong underwater adhesion of the patterned hydrogels to the beef heart tissue.

Movie S5

Underwater debonding of PA hydrogels on glass.

We recorded the debonding process of PA hydrogels in the underwater probe tack test for a flat P0 and a patterned P1 hydrogel on glass plates with a display speed 32 times faster than real time. For the flat hydrogel, only a small part of the surface was in contact with the glass plate due to water trapping acting as flaws, therefore the crack easily propagated during the debonding process. For the P1 hydrogel, all the hexagonal facets quickly made contact with the glass, and each hexagonal pillar significantly deformed before debonding. Each pillar debonding required re-initiation of the crack, resulting in a delayed debonding. The large deformation caused the PA hydrogel to dissipate a large amount of energy before the failure of the bonding joint, contributing to the debonding energy.

Movie S6

Underwater debonding of PA hydrogels on flat PA hydrogel.

We recorded the debonding process of PA hydrogels in the underwater probe tack test for flat P0 and patterned P1 hydrogels on the flat PA hydrogel. The speed was 32 times faster than real time. For the flat hydrogels, similar to their debonding on glass, only a small part of the surface was in contact with the hydrogel due to water trapping acting as flaws. Therefore, the crack easily propagated during the debonding process. For the P1 hydrogel, most of the pillars could be significantly stretched. Compared with the rigid glass substrate, the flat and soft PA

substrates could be stretched, which also contributed to the debonding energy. The PA hydrogel was so tough that, even the substrate was stretched a lot, the bonding joint detached from the interface.

3. Supplementary Figures

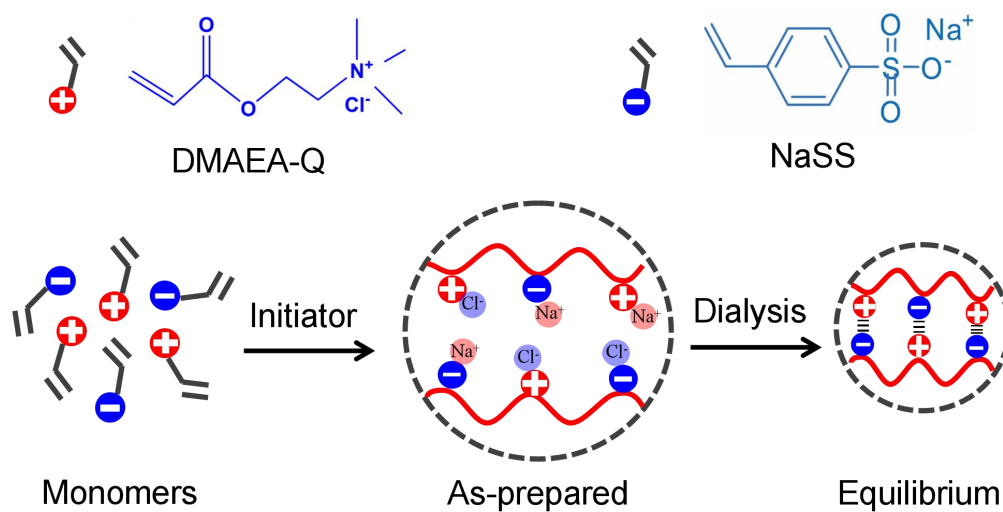


Figure S1. Schematic illustration of the polyampholyte (PA) hydrogels synthesis.

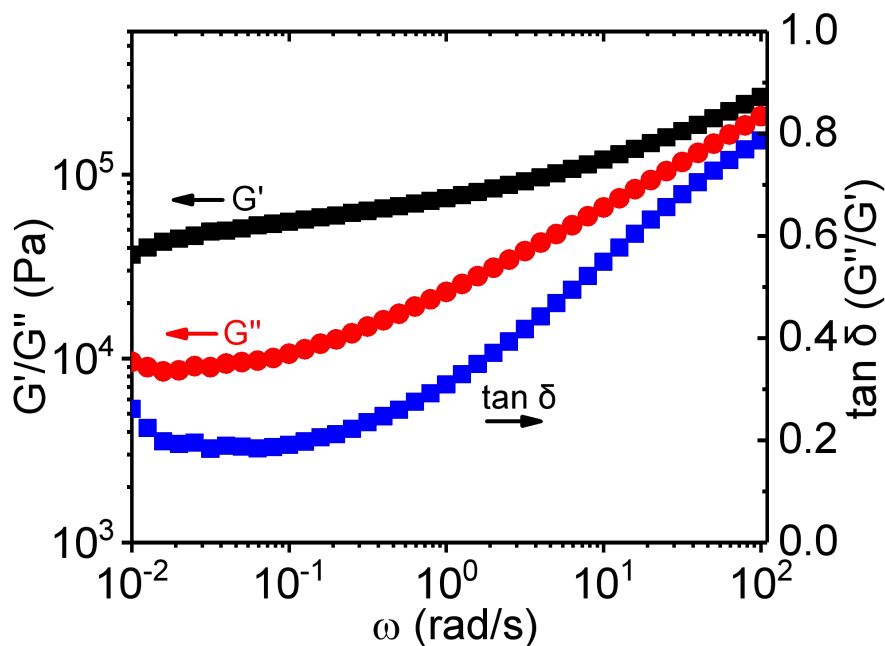


Figure S2. Rheological characterization of the PA hydrogel at 25 °C. G' , G'' , and $\tan \delta$ represent the storage and loss modulus, angular frequency and loss factor, respectively.

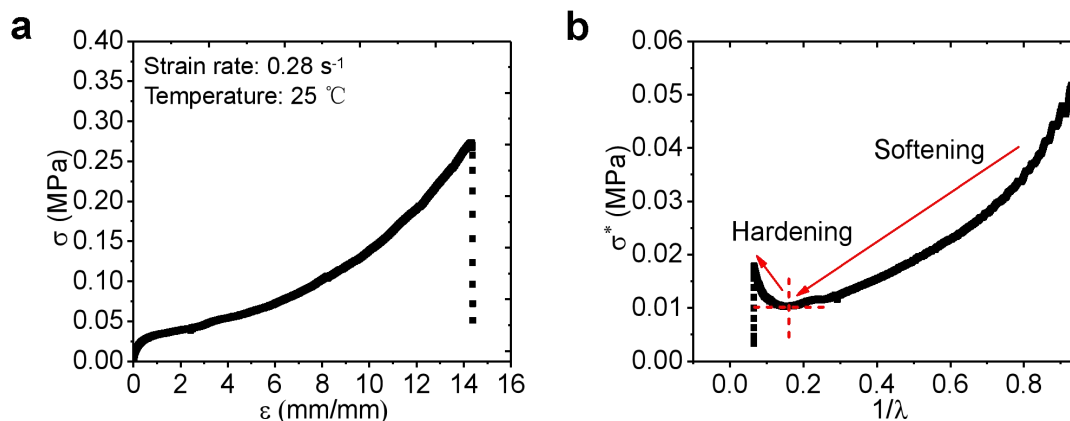


Figure S3. Tensile behavior of the PA hydrogel. a) Nominal stress (σ) vs. strain (ϵ) curve. b) Mooney representation of the same data as a function of $1/\lambda$, where $\lambda = \epsilon + 1$ is the deformation ratio. The reduced stress also called Mooney stress is defined as $\sigma^* = \sigma/(\lambda - \lambda^{-2})$. The mechanical properties of the hydrogel are characterized using the underwater tensile test at a steady 0.28 s^{-1} loading strain rate at 25 °C.

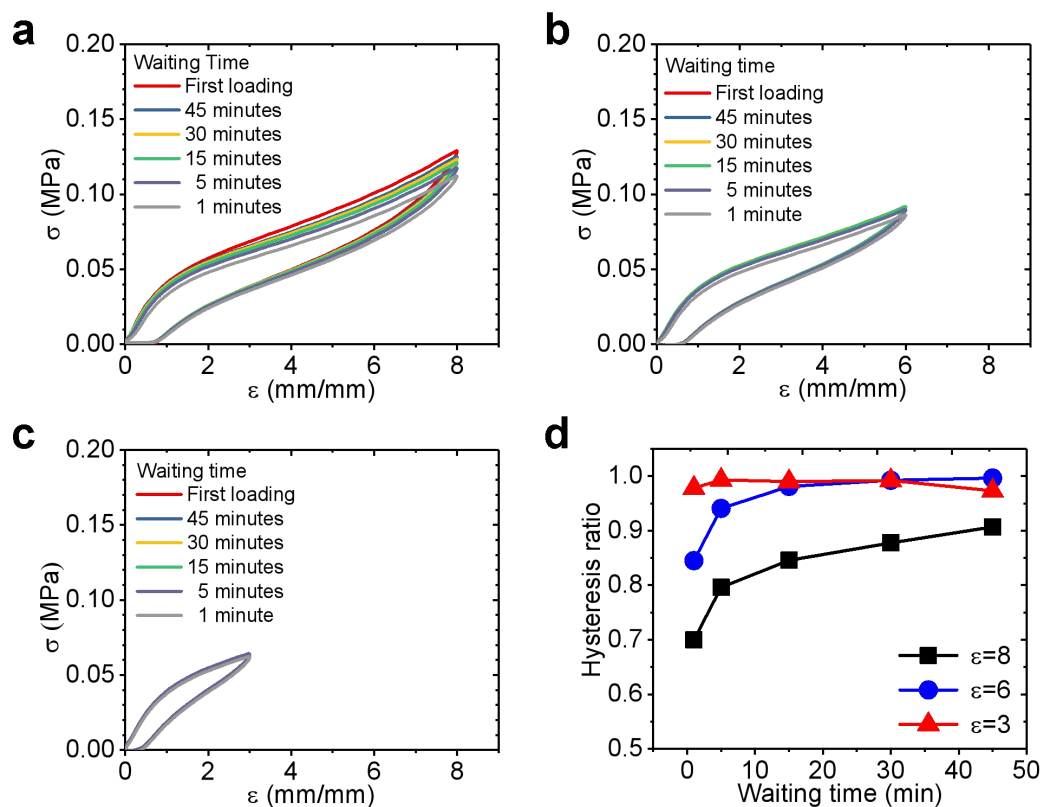


Figure S4. Mechanical hysteresis tests of the PA hydrogel. a–c) Nominal stress (σ) vs. strain (ϵ) cyclic tensile curves for different waiting times (t) at different maximum stretch strains (ϵ). d) Hysteresis ratio vs. waiting time curves for different maximum stretch strains. The tests were performed underwater at a 0.28 s^{-1} strain rate.

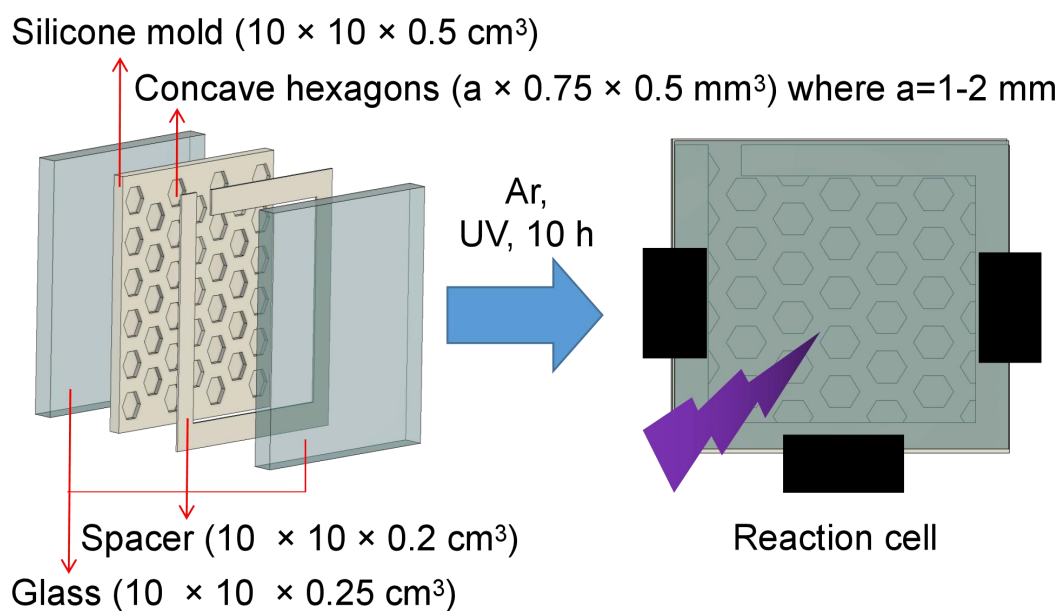


Figure S5. Schematics for the synthesis of the surface patterned hydrogel. A reaction cell was prepared by assembling two glass plates, a silicone mold with honeycomb ridges and a

silicone spacer. The precursor solution was added to the reaction cell, and after removing the bubbles in an argon atmosphere, the reaction cell was irradiated with UV light (365 nm wavelength) for 10 h to obtain the solidified hydrogel. The side length of each hexagonal concave area of the silicone mold varied from 1 to 2 mm, while the depth was 0.5 mm.

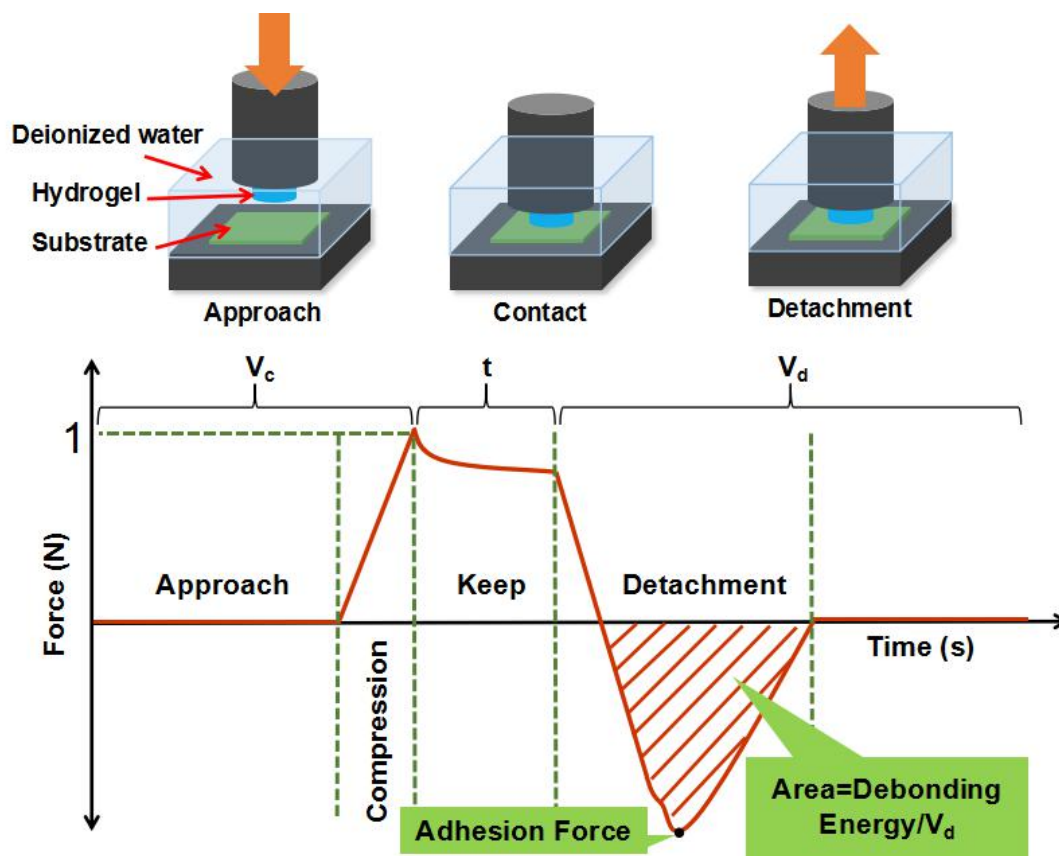


Figure S6. Schematics for the set-up and procedures of the underwater probe tack test. The hydrogel sample was fastened to the jigs and the system immersed in deionized water. The jig approached the substrate at a steady $V_c=10 \mu\text{m/s}$ rate until the applied force reached 1 N and subsequently held the position for 10 s. Afterward, the jig retracted at a steady $V_d=10 \mu\text{m/s}$ rate. The adhesion strength was calculated from the ratio of the debonding peak force to the projected area of the sample surface. The debonding energy per unit area was calculated from the ratio of the area under the force-displacement curve to the projected area of the sample surface.

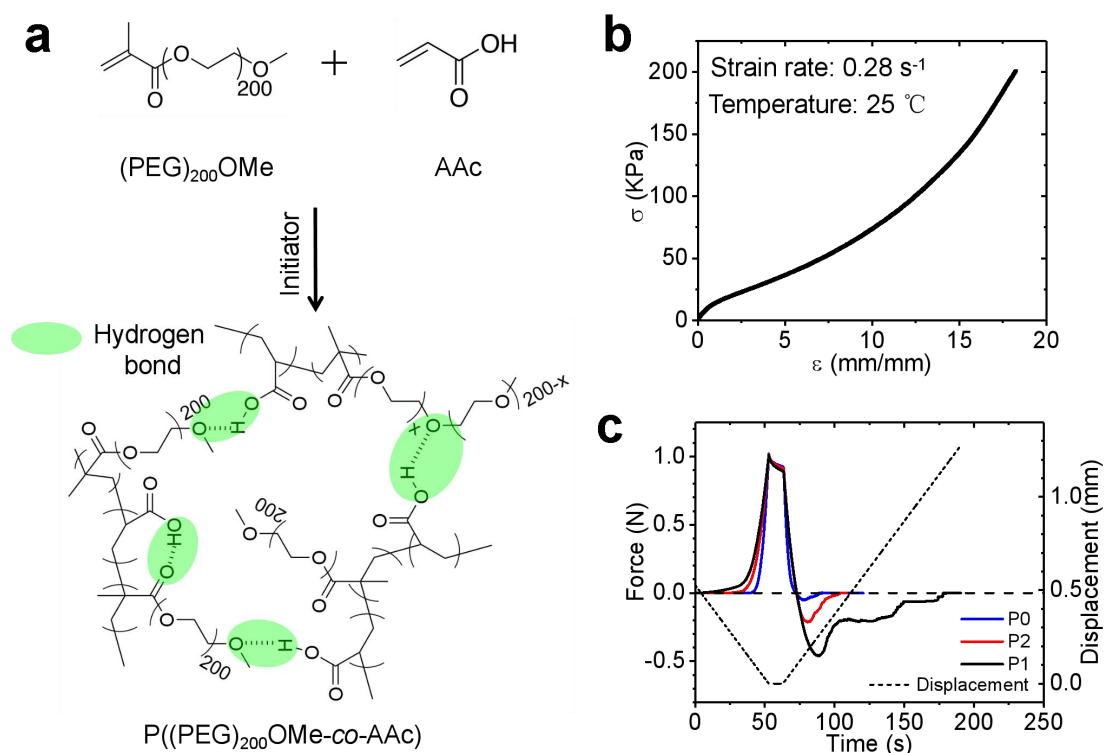


Figure S7. Underwater adhesion of the surface engineered hydrogel with hydrogen bonding. a) Chemical structures of $(\text{PEG})_{200}\text{OMe}$, AAc, and their copolymer $\text{P}((\text{PEG})_{200}\text{OMe-co-AAc})$, denoted as POA, formed by radical initiated polymerization. The POA forms hydrogels by hydrogen bonding. b) Tensile behavior of the hydrogen bonded hydrogels. c) Displacement-time and force-time profiles of the underwater tack test of the hydrogen bonded hydrogels with different surface patterns on glass. The sample code and dimensions of the pattern are shown in Table S2. The a , h , w , and t parameters correspond to those shown in Figure 1f.

4. Supplementary Tables

Table S1. Structure parameters of surface engineered PA hydrogels. The PA hydrogels deswelled to 87.5% of their as-prepared size in each direction in water.

Sample code	Length of hexagonal facet a (mm)	Height of hexagonal facet h (mm)	Groove width w (mm)	Total thickness $h+t$ (mm)	Relative area of hexagonal facets
P1	0.875	0.438	0.656	2.19	53%
P2	1.75				71%
P0 (flat)	-	-	-	2.19	100%

Table S2. Structure parameters of the surface engineered POA hydrogels.

Sample code	Length of hexagonal facet a (mm)	Height of hexagonal facet h (mm)	Groove width w (mm)	Total thickness $h+t$ (mm)	Relative area of hexagonal facets
P1	0.81	0.41	0.61	2.03	53%
P2	1.62				71%
P0 (flat)	-	-	-	2.03	100%

5. Supplementary References

- [1] T. L. Sun, T. Kurokawa, S. Kuroda, A. B. Ihsan, T. Akasaki, K. Sato, M. A. Haque, T. Nakajima, J. P. Gong, *Nat. Mater.* **2013**, *12*, 932.
- [2] T. Yamaguchi, K. Koike, M. Doi, *Europhys. Lett.* **2007**, *77*, 64002.
- [3] H. Lakrout, P. Sergot, C. Creton, *J. Adhesion* **1999**, *69*, 307.
- [4] R. Ulrich, R. T. Torge, *Applied Optics* **1973**, *12*, 2901.